Journal of the European Ceramic Society **18** (1998) 487–493

PII: S0955-2219(97)00161-1
0955-2219/98/$19.00 + 0.00

Influence of Solid Loading on Drying-Shrinkage Behaviour of Slip Cast Bodies

Giuliano Tarì and José M. F. Ferreira

Department of Ceramics and Glass Engineering, University of Aveiro, 3810 Aveiro, Portugal

(Received 4 June 1997; accepted 11 August 1997)

Abstract

Drying-shrinkage behaviour, described by Bigot's curves, was used to characterise slip cast bodies prepared from suspensions at different solid loading and dispersed with polyelectrolyte type surface active agents. Various ceramic materials (alumina, silicon carbide and calcium carbonate) were examined in order to establish a general relationship among solid loading of the starting suspension, particle packing in green state and drying behaviour. The Bigot's curves indicated that the shrinkage decreases with increasing solids' concentration, whereas the critical moisture content (CMC) shows an initial decrease followed by a trend towards a constant value at higher solid loading. The slope of the straight lines corresponding to the first stage of drying first increases with augmenting solid concentration, but decreases again for high solid loading. For all materials tested, good relationships were found between the CMC and slip cast density (correlation coefficients higher than 0·98) as well as between the shrinkage during the first stage of the drying process and solid loading (correlation coefficients higher than 0·99). Finally, Bigot's curves revealed to be a very simple yet effective tool to characterise the porous microstructure of slip cast bodies. In contrast, evaluation of the pore size distribution in relative dense slip cast bodies by Hg-porosimetry was found to be a less reliable method. © *1998 Elsevier Science Limited. All rights reserved*

1 Introduction

Drying-shrinkage behaviour, as given by Bigot's curves, is normally used as routine control in traditional ceramic production for testing the sensibility of clays and pastes to drying.[1,2] However, this paper demonstrates that the Bigot's curves can also be extended to the technical ceramic field and used as a powerful tool to characterise slip cast bodies. Drying-shrinkage behaviour, indeed, permits an accurate and complete characterisation of slip cast bodies, giving complementary information to respect Hg porosimetry.[3,4]

In this study, Bigot's curves were used to study the influence of solid loading on the porous microstructures of slip cast bodies. Three ceramic materials (alumina, silicon carbide and calcium carbonate) were dispersed in water with two organic surface active agents (Dolapix CE64 and Targon 1128). Suspensions at different solid loading were prepared and the particle packing ability during slip casting evaluated by analysing the drying-shrinkage behaviour of the green compacts, as well as their density and pore size distribution.

2 Background

The main steps of the drying process of a saturated porous structure can be described as follows.[5] Initially, the saturated body exhibits a loss of moisture content accompanied by a shrinkage, during which free-liquid evaporates from the external surface of the compact. Consequently, the particles approach each other and the shrinkage is proportional to the weight loss. This first step of the drying process is normally called constant-rate period, because the rate of evaporation per unit area of the drying surface is independent of time. Some liquid remains between particles (interstitial liquid) and no air is admitted into the system at this stage. As drying continues, the liquid evaporated is continuously replaced by other liquid drawn from the internal pores to the surface by capillary action until the particles establish mutual contacts and the so-called critical moisture content (CMC) is reached. Figure 1 represents a typical Bigot's curve, in which the shrinkage of the wet body is plotted as a function of its moisture

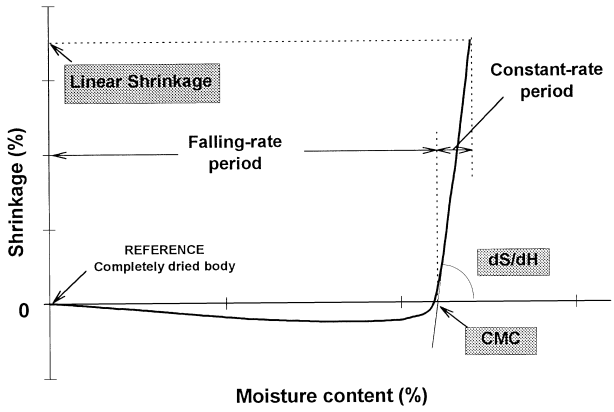

Fig. 1. The main features of the Bigot's curves.

content.[1,2] The CMC is defined as the intercept with the moisture content axis of the straight lines corresponding to the constant-rate period. After the CMC, the rate at which the liquid is evaporated from the surface is greater than the rate at which it is replaced and thus, the overall rate of drying decreases. In this second stage of the drying process, usually called falling-rate period, the escape of liquid is not associated with shrinkage and air enters into the body. Consequently, air replaces the liquid that still fills the internal pores (interstitial liquid), diminishing the moisture content of the body from CMC to the equilibrium moisture content. Besides the CMC, other important features of the Bigot's curves are the total shrinkage and the slope, dS/dH, (where S and H stand for shrinkage and moisture content, respectively). A final expansion of the body after the CMC is also commonly observed.[3] All these features of the Bigot's curves will depend on the pore size distribution and, hence, on the particle packing.

Dimensional changes suffered by the porous structure during drying are due to stresses derived from temperature and moisture gradients existing within the body and from the capillary forces.[6] The first ones produce differential volume changes with heating, due to differential thermal expansion of the components inside the body and moisture removal. The capillary suction forces are connected with the wetting properties of the solid by the liquid, and with the porous structure of the wet body. If shrinkage took place uniformly, as can be approximately considered in relative dense slip cast bodies, the strain behaviour will be quite simplified since the shrinkage is related only to the capillary mechanism. The capillary theory describes the equilibrium forces established at the interfaces among solid, liquid, and vapour phases, originated from differences in surface energies. As the water is progressively removed from the wet body, this difference in surface energy causes an increase of the curvature of water surface in the interstices (menisci) and a suction pressure is set up. The suction pressure across these curved surfaces, ΔP, tends to draw liquid from the interior to the surface and, for a liquid that completely wets the solid phase, the relation is expressed by:[5,7]

$$\Delta P = -2\gamma_{LV}/r \tag{1}$$

where γ_{LV} represents the surface tension for contact between liquid and vapour phases and r the radius of the menisci. Equation (1) clearly indicates that, beyond the chemical and physical nature of the phases involved in the process, the drying of a particulate system depends upon the pore size, since the capillary stress depends on the radius of the interconnected pores. From eqn (1), it can also be depicted that when the centre of the curvature is in the vapour phase, the radius of the menisci is negative and the liquid is in tension ($\Delta P > 0$). This tension corresponds to the compressive force responsible for the shrinkage of the system.

Figure 2 schematically shows the evolution of the liquid-vapour interface during the constant-rate

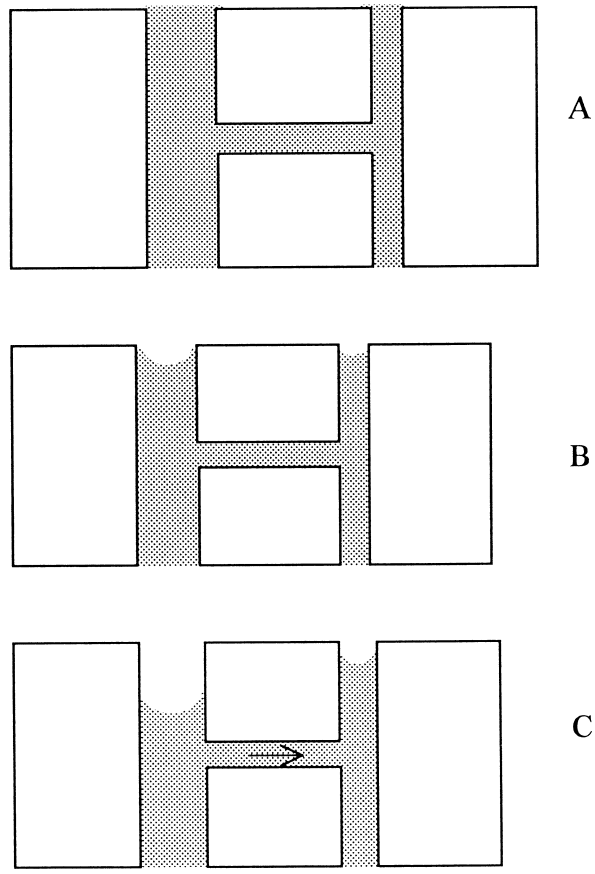

Fig. 2. Schematic of a green body having different pore sizes: (a) saturated body in which the menisci are flat; (b) constant-rate period during which the radius of the menisci are independent to the radius of the pores; (c) falling-rate period during which the liquid is drained from the larger pores by the smaller ones.

period for a green body having different pore sizes. At first, the liquid forms a continuous film covering the surface [Fig. 2(a)]. However, when the surface becomes scarce of liquid, menisci start to form. At this stage, the curvature of menisci is constant regardless of the pore sizes present in the sample [Fig. 2(b)]. When the radius of the curvature of the menisci equals the larger pore radius, evaporation continues preferentially from the menisci of finer pores due to the higher capillary force exerted by them [Fig. 2(c)]. In this way, larger pores are emptied first, whereas smaller pores remain full of liquid. This means that when CMC is reached, the larger pores could have already been emptied and the value measured should be lower than expected from pore volume fraction. For the same reasons, the drying of a green body with a broader pore size distribution will occurs at a lower shrinkage rate, dS/dH, compared with another having a more uniform pore size distribution, since the driving force for shrinkage is smaller in larger pores and their contribution to weight loss is higher.

3 Experimental Procedure

3.1 Materials and slip preparation

Three commercial ceramic powders were used in this study: alumina (A16 SG, Alcoa Chemicals, USA), silicon carbide (NF1, Elektroschmelzwerk Kempten GmbH, Germany) and calcium carbonate (Mα, Mineraria Sacilese, Italy). Figure 3 shows the particle size distribution (SediGraph 5100, Micrometrics, USA) of the three starting powders. The dispersants used were a polyacrylic acid (Dolapix CE 64, Hans Barnstorf & C., Germany) for the alumina suspensions and an ammonium polycarbonate (Targon 1128, BK Ladenburg, Germany) for the silicon carbide and calcium carbonate suspensions. Both these dispersants act through electrosteric interactions and were chosen because of their high efficiency in stabilising high concentrated suspensions.[3,4,8] Preliminary deflocculation curves were performed in order to determine the minimum amount of dispersant that gave the less viscous slips.

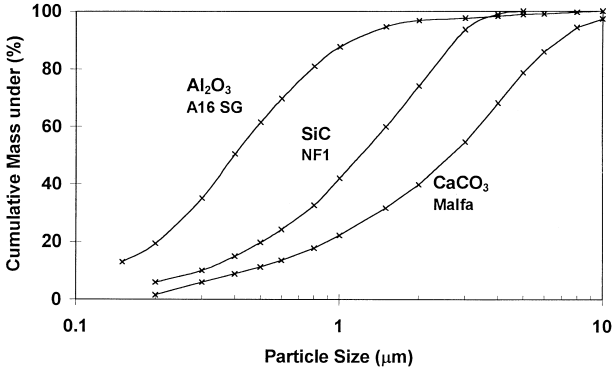

Fig. 3. Particle size distributions of the starting powders.

According to the dispersion performance of each material, aqueous suspensions at different solid loading (from 30 vol% up to 55 vol% for SiC and 60 vol% for Al_2O_3, and $CaCO_3$) were prepared by first mixing dispersant and water. Then, while stirring, the powders were added and the resulting suspension was kept stirred for a further 30 min. Deagglomeration and homogenisation were performed by ball milling in a plastic container for 12 h with cylindrical grinding media. After milling, the slip was conditioned for 6 h, by rolling in the plastic containers without balls, in order to stabilise the slip's properties.

3.2 Preparation and characterisation of the green body

The drying-shrinkage behaviour of the green compacts obtained from suspensions at different solid loading was determined by using a barelatographe (Adamel Lhomargy, France), a mechanical device that simultaneously measures the variation of weight and length of the sample during drying. Solid cast bars (length= 11 mm, trapezoidal section with area $[15(15+17)/2]\,mm^2$) were obtained by slip casting into suitable plaster moulds. Just after demoulding, two pieces of approx. 40 mm were cut, weighed and carefully placed in the barelatographe for the simultaneous measurement of shrinkage and weight loss. The natural drying (at RT) of the samples was recorded for one day and, after that, the drying was completed in a stove at 120°C for 12 h. The weight and length of the completely dried samples were measured and used as reference for plotting the Bigot's curves. The intercept, CMC, and the slope, dS/dH, were determined using a linear regression of the data (at last three points) in the first stage of drying.

The relative density of the slip cast samples was measured by the Archimedes principle using a mercury balance. Finally, the pore size distribution was determined by Hg intrusion porosimetry (PoreSizer 320, Micromeritics, USA). The high pressure part of each experiment was carried out using the automatic mode with an equilibration time of 10 s at each point. The surface tension and contact angle adopted were $48{\cdot}5\ 10^{-2}$ N m^{-1} and 130°, respectively.[9]

4 Results and Discussion

The Bigot's curves of the green bodies prepared from slips at different solid loading are reported in Fig. 4(a)–(c), for alumina, silicon carbide and calcium carbonate, respectively. Alumina and silicon

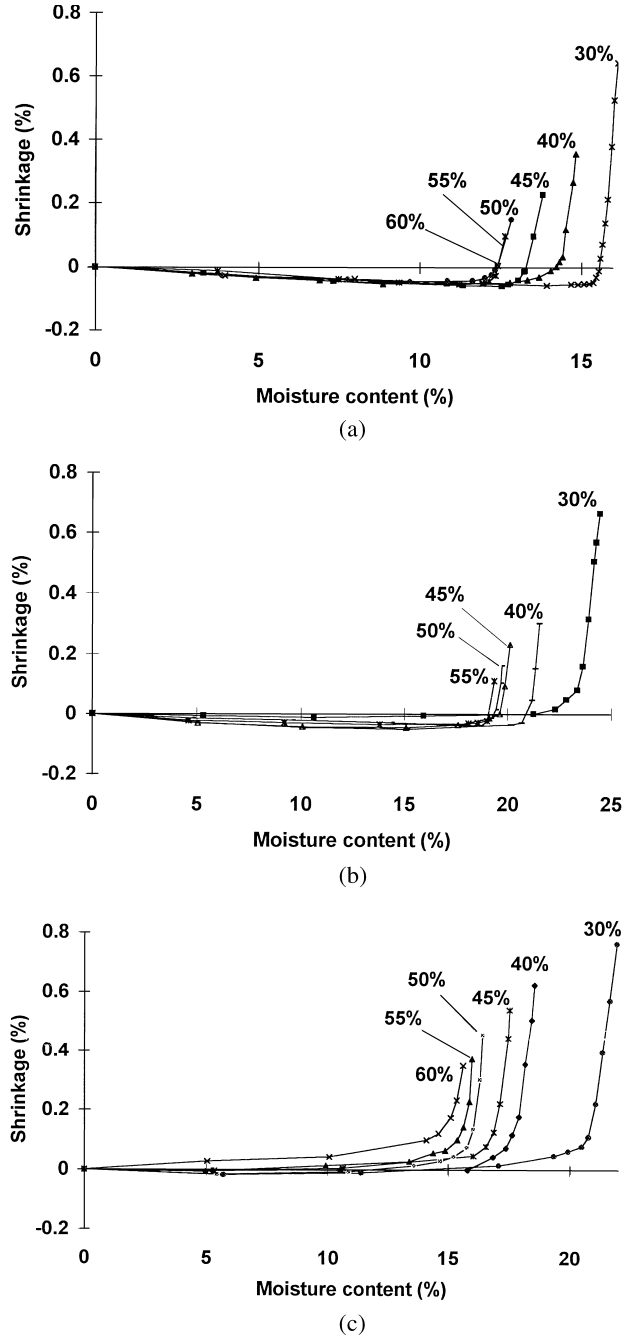

Fig. 4. Bigot's curves of the slip cast bodies obtained from (a) alumina, (b) silicon carbide, (c) calcium carbonate suspensions at different solid loading.

carbide samples present similar drying-shrinkage behaviours and expansion after CMC, whilst the calcium carbonate samples exhibit a secondary shrinkage after CMC that becomes more pronounced with increasing solid loading. This secondary shrinkage may derive from a slow approximation between flatly surfaces, resulting from the preferential cleavage directions of calcite that will occur during milling. SEM micrographies, indeed, revealed the typical polyedral aspect of the calcite particles.[8] Since the particles in green compacts are randomly oriented, there will exist both point to point and face to face contacts. These face to face contacts give rise to thin and extended liquid films, that still persist after CMC and a gradual approximation between these surfaces will occur during the falling rate period. This phenomenon is commonly observed in layered structured materials such as montmorillonite.[10] The main features of Bigot's curves are summarised in Table 1, together with the relative density (expressed as percentage with respect to the theoretical density) and some representative porosity data of the dried samples.

Figure 4 and Table 1 clearly show a continuous decrease of linear shrinkage and CMC of the slip cast bodies with increasing solid contents. The evolution of CMC can be more easily appreciated from Fig. 5. In the case of calcium carbonate the decreasing trend is observed over all solid loading range tested, whereas for the other materials the CMC gets up a 'critical value' at higher solid loading. These variations appear closely related to the packing ability of the powders as determined by the particle size and particle size distributions.[3,4,8] Since the CMC is expressed as a wt% of water (dry basis), it also depends upon particle density. This explains why the more relatively dense calcium carbonate slip cast bodies have higher CMC values than alumina samples, although the secondary shrinkage ($CaCO_3$) and the expansion (Al_2O_3) after CMC also contribute to the observed difference. The results presented show that a decrease in both CMC and linear shrinkage are normally accompanied by increments in relative density, and vice versa.

Among the features of the Bigot's curves, the slope of the straight lines corresponding to the first stage of the drying represents the most difficult parameter to measure accurately, especially at high solid loading when the linear shrinkage becomes very small. Despite these difficulties, the variation of the slopes with solid loading revealed a quite interesting trend, as can be noticed from Table 1. For the coarser SiC and $CaCO_3$ powders, dS/dH first increases until reaching maximum values,

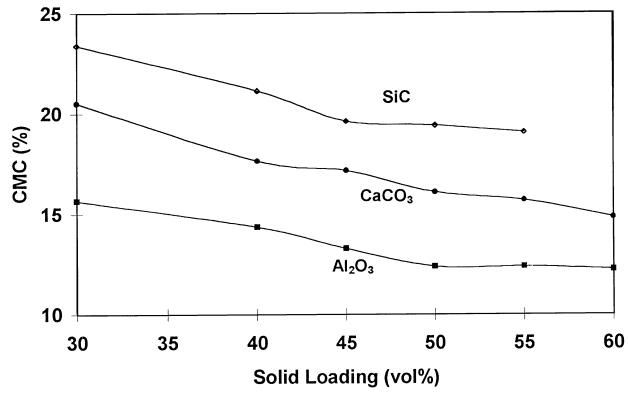

Fig. 5. Evolution of CMC with solid loading. ●, $CaCO_3$; ✧, SiC; ■, Al_2O_3.

Table 1. Drying-shrinkage features, main porosity data and relative density of the slip cast bodies at different solid loading. The theoretical density was assumed to be 2·71, 3·21 and 3·98 g cm^{-3} for $CaCO_3$, SiC and Al_2O_3, respectively

		Solid contents (%)					
		30	*40*	*45*	*50*	*55*	*60*
Al_2O_3	CMC (%)	15·7	14·4	13·3	12·4	12·4	12·2
	Linear shrinkage (%)	0·66	0·36	0·23	0·15	0·10	0·06
	dS/dH	1·16	0·61	0·44	0·34	0·42	—
	TD (%)	61·6	64·1	65·8	66·0	66·3	66·8
	Total pore volume (ml g^{-1})	0·083	0·132	0·140	0·131	0·120	0·123
	Median pore diameter[a] (μm)	0·061	0·053	0·057	0·056	0·056	0·059
SiC	CMC (%)	23·4	21·1	19·6	19·4	19·1	—
	Linear shrinkage (%)	0·66	0·31	0·23	0·16	0·11	—
	dS/dH	0·41	0·76	0·46	0·46	—	—
	TD (%)	55·8	60·1	61·7	632·3	62·9	—
	Total pore volume (ml g^{-1})	0·217	0·210	0·188	0·105	0·100	—
	Median pore diameter[a] (μm)	0·172	0·163	0·157	0·151	0·142	—
$CaCO_3$	CMC(%)	20·5	17·7	17·2	16·1	15·7	14·8
	Linear shrinkage (%)	0·77	0·63	0·43	0·46	0·38	0·35
	dS/DH	0·57	0·68	0·63	0·78	0·60	0·47
	TD(%)	63·5	67·9	68·6	69·0	72·0	73·4
	Total pore volume (ml g^{-1})	0·157	0·090	0·083	0·156	0·173	0·133
	Median pore diameter[a] (μm)	0·114	0·161	0·151	0·183	0·114	0·174

[a]Based on volume of mercury intruded.

followed by a decreasing trend at higher solid contents. In contrast, the finer alumina powder only displays the decreasing part.

In slip cast bodies prepared from well-dispersed slurries, the linear shrinkage is directly connected with the thickness of liquid layers surrounding the particles.[4,11] An increasing number of particles in suspension sharing the same amount of liquid leads to a higher frequency of mutual collisions and overlapping of their electrical double layers. Hence, a reduction of the hydrated layer thickness around each particle is expected, leading to a closer mutual approach in suspension as well as in the wet body.[4] To better explain this concept, let us consider a suspension formed by monosized particles having diameter d and a solid volume fraction φ. In a first approximation, we can assume that all the liquid phase present, (1-φ), is expended in the formation of the hydrated layers of thickness δ, surrounding the particles. The volume of the liquid layer surrounding each particle (V_δ) is given by:

$$V_\delta = \pi/6\left[(d+2\delta)^3 - d^3\right] \tag{2}$$

The solid loading can be related to d and δ by the following expression:

$$\varphi = V_d/(V_\delta + Vd) = d^3/(d+2\delta)^3 \tag{3}$$

where V_d is the volume of a spherical particle of diameter d.

If instead of monosized spheres, we consider a system composed of spheres having different sizes, d_1, d_2, d_n, and combined in different volume fractions, x_1, x_2, ...x_n, the total solid loading will be given by:

$$\begin{aligned}\varphi &= x_1 V_{d1}/(V_\delta + V_{d1}) + x_2 V_{d2}/(V_\delta + V_{d2}) \\ &\quad + \ldots + (1 - x_1 - x_2 - \ldots x_n) V_{dn}/(V_\delta + V_{dn}) \\ &= x_1 d_1^3/(\delta + d_1)^3 + x_2 d_2^3/(\delta + d_2)^3 + \ldots \\ &\quad + (1 - x_1 - x_2 - \ldots - x_n) d_n^3/(\delta + d_n)^3\end{aligned} \tag{4}$$

During consolidation some water is removed by the plaster mould. Consequently, the solid volume fraction increases and the thickness of the hydrated layers will be reduced. However, the same dependence on solid loading will be maintained, as suggested in Fig. 6, which reports the solutions of eqns (3) and (4), in terms of thickness of hydrated layers

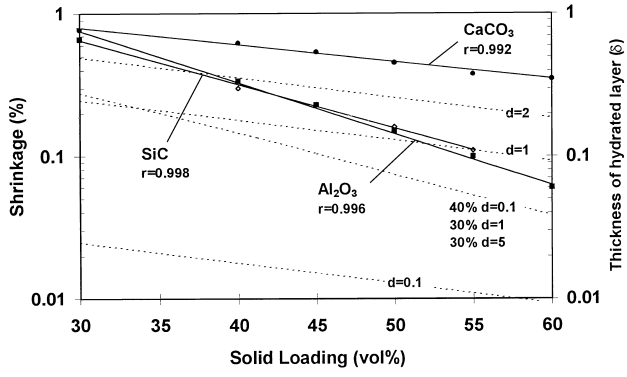

Fig. 6. Correlation between solid loading, the measured linear shrinkage values (continuous lines), and the estimated thickness of the hydrated layers, from eqns (3) and (4), for various uniform particle sizes and discrete particle size distributions (dashed lines). ●, $CaCO_3$; ◇, SiC; ■, Al_2O_3.

(dashed lines), for different values of *d*, over the all solid loading range tested. The correspondent measured shrinkage in the consolidated bodies is also represented and these experimental points were joined by trend lines (continuous lines). As expected, both shrinkage and thickness of hydrated layers display a similar evolution as a function of solid loading with very high values for the correlation coefficients. Further, a close relationship between shrinkage and particle size distribution also appears evident from Fig. 6. In fact, the relative positions and the slopes of the experimental curves are in close agreement with the particle size and particle size distributions of the starting powders (Fig. 3).

The dependence of CMC (and dS/dH) on solid loading derives from two contradictory effects. An increasing number of particles in suspension leads to: (i) a closer mutual approach and thus, to a higher cast density in the wet state; (ii) a less efficient powder dispersion that can lead to formation of agglomerates and, thus, to a decreased ability to pack. At low solid loading, thick electrical double layers can be formed around the particles. The average distance between particles will be higher, either in suspension as well as in the green body, compared with the situation that should occur when starting from more concentrated suspensions.[4] Diluted slips having higher fluidity are also more prone to particle segregation phenomena, especially when coarse particles are present. Particle segregation will lead to broader pore size distributions. This explains the higher CMC values observed for green bodies cast from the more diluted slips, as well as the lower slopes dS/dH observed for the coarser powders. For the finer alumina powder, the settling of particles will be reduced, even from the more diluted suspensions. In these conditions, the slow consolidation rate would enable the formation of a high ordered particle packing and a narrow pore size distribution that might result in the high dS/dH values observed.

Slip casting performance gradually improves with increasing solid volume fraction. However, at very high solid loading, suspensions become too crowded and the thickness of the hydrated layer becomes inevitably reduced. Hence, the average interparticle distance in suspension is shorter than in the earlier situation and both the frequency of particle collisions and the deposition rate significantly increase. Particles have not enough time to search for a favourable position in the cake being formed, and a less ordered particle packing may occur.[12] This explains why the slope dS/dH tends to decrease again for high solid loading. The same reasoning can be used to explain why the CMC tends to constant values with solid loading increasing, in the case of powders with a lower packing ability (SiC, Al_2O_3). With the calcium carbonate, the CMC appears to decrease continuously with the solid loading, without attaining any plateau. This is probably due to the higher packing ability of this powder due to a more favourable particle size distribution. Hence, more water will be available to thicken the hydrated layers around particles, as can be also noticed from the overall higher shrinkage of calcium carbonate samples.

Figure 7 confirms the close correlation existing between packing density and the CMC values, with very high correlation coefficients. The correlation between CMC and slip cast density is not surprising and can be explained as follows:[3] if particles were spherical, uniform in size, and formed a regular packed structure with a uniform pore size, the CMC should represent the amount of water filling the interstitial pore space when particles touch each other. However, real systems do not fulfil these ideal requirements. Particle shapes other than spherical, particle size distribution, segregation phenomena at lower solids' concentration, mutual interference of particles during the deposition stage, stabilisation degree and stabilising mechanism are determining factors of the porous microstructures. The porous structure, in turn, influences the drying-shrinkage behaviour. Larger pores containing higher volumes of liquid phase will have a smaller contribution to the shrinkage (dS) and a significant influence in the weight loss (dH). Further, the capillary tensions are inversely proportional to the pore radius.[5,7] Accordingly, the coarser pores will be emptied by the finer ones, before the CMC [Fig. 2(c)], and the slope of the straight lines corresponding to the first stage of drying dS/dH will decrease. So, even if the shrinkage and the loss of moisture content of a saturated and deformable structure having non-uniform pore sizes were linearly related in the first stage of the drying process, the slope will decrease faster than in the ideal case of uniform pore size. The draining

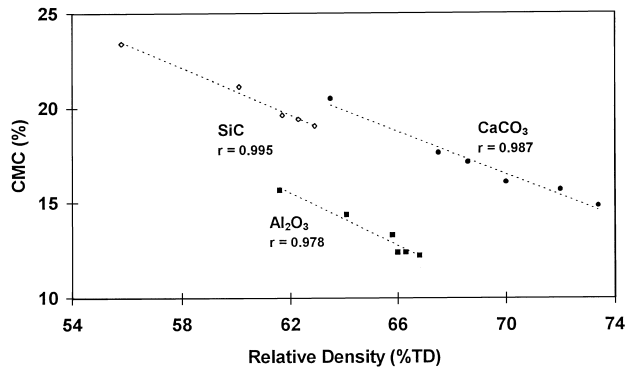

Fig. 7. Correlation between CMC and relative density of the slip cast bodies.

of coarser pores by the smaller ones will result in lower CMC values.

According to the discussion above, broadening of pore size distribution should occur for the solid contents higher than a 'critical' value at which the CMC becomes almost constant. The porosity data presented in Table 1 roughly confirms this trend. However, porosity data also show some disagreements between total pore volume and green density, especially for the $CaCO_3$ samples. Some porosity measurements were repeated two or three times in order to test the reproducibility of this method. It was concluded that the observed differences are within the experimental error. On the other hand, the density measurements showed a high reliability. Besides the classical sources of error of mercury porosimetry technique,[9,13] such as non-cylindrical pore shapes, non-interconnectivity between pores, interaction between test material and mercury, existence of trapped gas etc., the difference in reproducibility of the measurements performed by these two techniques may also derive from the low total pore volume and from different sizes of the samples tested, about 7–10g (density) and 1·0–1·7 g (porosimetry).

5 Summary and Conclusion

- The total shrinkage of the slip cast bodies always decreases with increasing solid loading in suspension. This was attributed to thinner hydrated layers surrounding the particles both in suspension and in the wet body. Close relationships between shrinkage versus solid loading (with correlation coefficients higher than 0·99) and shrinkage versus particle size distribution were found.
- The CMC of the slip cast bodies tends to decrease with increasing solid contents. In the case of calcium carbonate, the decreasing trend was observed over the all solid loading range tested, whilst for other materials the CMC gets up a 'critical value' at higher solid loading. These variations appear closely related with the packing ability of the powders, as can be also verified by the relationship existing between CMC and packing density with correlation coefficients higher than 0·98. The slopes of the straight lines of the Bigot's curves (dS/dH) corresponding to the first stage of the drying give information about pore size distribution within the consolidated bodies and, in some way, also affects the CMC values.
- Overall, drying-shrinkage behaviour, as given by the Bigot's curves, revealed to be a very simple and powerful tool to characterise the structure of slip cast bodies.

Acknowledgements

This work was supported by the JNICT Project no. PBIC/C/CTM/1968/95. The authors also acknowledge Mrs F. Neves Cruz for carrying out some of the experimental work.

References

1. Bigot, A., *Retrait au Sechage des Kaolins et Argiles*, Report of Academy of Sciences, Paris, 1921.
2. Aliprandi, G., *Principi di Ceramugia e Tecnologia Ceramica*, E.c.i.g., Genova, 1975.
3. Ferreira, J. M. F., A interface SiC–Soluşão aquosa e o enchimento por barbotina. PhD thesis, University of Aveiro, Portugal, 1992.
4. Tarì, G., Ferreira, J. M. F. and Lyckfeldt, O. 'Influence of stabilisation mechanism and solid loading on slip casting of alumina, Submitted to *J. Europ. Ceram. Soc.*
5. Foust, A. S., Wenzel, A. W., Clump, C. W., Maus, L. and Andersen, L. B., *Principles of Unit Operations*, 2nd edn. John Wiley & Sons, New York, 1980.
6. Hasatani, M. and Itaya, Y., Drying-induced strain and stress: a review'. *Drying Technology*, 1996, **14**, 1011–1040.
7. Scherer, G. W., Theory of drying. *J. Am. Ceram. Soc.*, 1990, **73**, 3–14.
8. Tarì, G. and Ferreira, J. M. F., Colloidal processing of calcium carbonate, to appear in *Ceram. Intern.* 1997.
9. With de, G. and Glass, H. J., Reliability and reproducibility of mercury intrusion porosimetry. *J. Europ. Ceram. Soc.*, 1997, **17**, 753–757.
10. Roget, M., Le séchage des produits céramiques. *L'Industrie Céramique*, 1976, **691**, 17–48.
11. Ruys, A. J. and Sorrel, C. C., Slip casting of alumina. *Am. Ceram. Bull.*, 1996, **75**(11), 66–69.
12. Ferreira, J. M. F. and Diz, H. M. M., Effect of solid loading on slip casting performance of silicon carbide slurries. Submitted for publication in the *J. Am. Ceram. Soc.* 1997.
13. German, R. M., *Particle Packing Characteristics*. MPIF, Princeton, N.J. 1989, p. 285.